JOURNAL of
MATERIALS and MECHATRONICS:A

e-ISSN 2717-8811
JournalMM, 2025, 6(1), 241-248
https://doi.org/10.55546/jmm.1670702

Araştırma Makalesi / Research Article

Deposition Time Effects on Sb_2S_3 Thin Film Properties via Hydrothermal Method

Hasan KOSEOGLU*

* Iskenderun Technical University, ISTE Center for Science and Technology Studies and Research (ISTE-CSTSR), Hatay, Türkiye, ORCID ID: https://orcid.org/0000-0002-9869-2708, hasan.koseoglu@iste.edu.tr

Geliş/ Received: 06.04.2025; **Revize/Revised:** 05.05.2025 **Kabul / Accepted:** 16.05.2025

ABSTRACT: Antimony sulfide (Sb_2S_3) is a highly promising semiconductor for sustainable thin-film solar cells due to its favorable optical and electrical properties. In this study, Sb_2S_3 thin films were deposited on indium tin oxide (ITO) coated glass substrates using a hydrothermal deposition technique with varying deposition times to investigate the impact of deposition duration on the morphological, optical, and structural properties of the films. The analysis revealed that deposition time is highly effective in modifying the physical properties of Sb_2S_3 thin films. It was demonstrated that employing the deposition time at 8 hours led to the formation of uniform and highly crystalline Sb_2S_3 films with (hk1) preferred orientation, suggesting its potential utility in solar cells.

Keywords: Antimony sulfide, Hydrothermal deposition, Thin film solar cells

*Sorumlu yazar / Corresponding author: hasan.koseoglu@iste.edu.tr
Bu makaleye atıf yapmak için /To cite this article

Koseoglu, H. (2025). Deposition Time Effects on Sb_2S_3 Thin Film Properties via Hydrothermal Method. Journal of Materials and Mechatronics: A (JournalMM), 6(1), 241-248.

1. INTRODUCTION

The binary semiconductor antimony sulfide (Sb_2S_3) is increasingly studied for photovoltaic applications, driven by its simple chemistry, non-toxic nature, optimal bandgap (~1.7 eV), and high absorption coefficient (~10^5 cm^{-1}) (Kondrotas et al., 2018). However, a significant gap exists between its theoretical power conversion efficiency predicted by the Shockley-Queisser limit (Shockley and Queisser, 1961) and the current record of 8.2% (Deng et al., 2024) for fabricated Sb_2S_3 solar cells. Developing effective and scalable deposition methods is essential to maximize the efficiency of Sb_2S_3 solar cells, as these methods directly influence the film's morphology, structure, electrical characteristics, and defect levels. While various physical and chemical techniques are employed to produce high-quality Sb_2S_3 thin films, the hydrothermal method has emerged as a particularly promising approach. Its advantages, including low-cost, low-temperature processing, precise control over film properties, and high reproducibility (Wang et al., 2020; Liu et al., 2016; Tang et al., 2020; Chen and Chen, 2020), have led to the current record power conversion efficiency for Sb_2S_3 solar cells (Deng et al., 2024).

Achieving effective hydrothermal deposition of Sb_2S_3 thin films depends heavily on the precise control of key reaction parameters, including temperature, deposition time, pressure, and precursor molarity, as well as post-annealing conditions, since the final film properties are directly influenced by these parameters (Vavale et al., 2018). Deposition time likely plays a dominant role in fine-tuning the properties of hydrothermally deposited thin films (Yildirim et al., 2019). It can also provide straightforward control over Sb_2S_3 thickness, which in turn affects both light absorption and charge carrier separation (Chen and Chen, 2020). Therefore, careful optimization of deposition time is essential to achieve Sb_2S_3 films with the desired uniformity, crystallinity, orientation, and optical characteristics for solar cells.

This study aimed to determine the relationship between deposition time and the resulting properties of Sb_2S_3 thin films, which were hydrothermally deposited at 135°C for 5, 8, 10, and 15 hours on ITO-coated glass substrates. The morphology, preferred orientation, and band gap of Sb_2S_3 thin films were thoroughly investigated as a function of deposition time. The study revealed that appropriate deposition times resulted in the formation of uniform and highly crystalline Sb_2S_3 films with (hk1) preferred orientation, indicating the potential of fabricated films for solar cells.

2. MATERIALS AND METHODS

Sb_2S_3 thin films were synthesized via hydrothermal deposition on SLG/ITO substrates (purchased from Teknoma Technological Materials Industrial and Trading Inc.). The precursor solutions were prepared by dissolving 20 mM antimony potassium tartrate ($C_8H_4K_2O_{12}Sb_2 \cdot xH_2O$, 99%) and 120 mM sodium thiosulfate pentahydrate ($Na_2S_2O_3 \cdot 5H_2O$, 99%) in 60 mL of deionized water. The solutions were magnetically stirred at 400 rpm to ensure homogeneity, and the pH values were determined to be 5.80 using a pH meter. Following solution preparation, the solutions were poured into a 100 mL Teflon-lined autoclave. SLG/ITO substrates were placed inside, ITO side down at a 75° angle. The autoclave was sealed, and Sb_2S_3 films were hydrothermally deposited at 135°C. Deposition times were varied at 5, 8, 10, and 15 hours to determine the optimal deposition time. Subsequently, the films were rinsed with deionized water, dried at room temperature, and annealed at 325°C in an argon environment, with a temperature ramp rate of 10 °C/min and a dwell time of 15 minutes. Samples fabricated at 5, 8, 10, and 15 hours were designated as S-5h, S-8h, S-10h, and S-15h, respectively.

The morphology and stoichiometry of the films were analyzed using a Thermo Fisher Scientific Apreo S Scanning Electron Microscopy (SEM). Surface topographies were visualized with a secondary electron detector (Everhart-Thornley Detector (ETD)) at 10 kV, 10 spot size, and 10 kX and 25 kX magnifications. Elemental compositions were determined via Energy-Dispersive X-ray Spectroscopy (EDS) technique at 30 kV, 10 spot, 10 kX magnification, and 10 mm working distance by Thermo Fisher Scientific UltraDry EDS Detector which was equipped with the SEM. The thicknesses of the films were measured from 50 kX cross-sectional SEM images. The crystal structure of the films was analyzed by X-ray Diffraction (XRD) using a Malvern Panalytical EMPYREAN diffractometer (Cu-K_α X-ray Tube, $\lambda_{x\text{-}ray}$=1.5406 Å, 2θ scan range: 10°-55°, Step size: 0.0262°, Scan speed: 2°/min). Energy Band gaps of the thin films were determined from UV-VIS transmission spectra (Wavelength scan range:1100-500 nm, Data interval: 2 nm, Scan Speed: 200 nm/min) using a Jasco/V-750 Spectrophotometer.

3. RESULTS AND DISCUSSION

3.1 Scanning Electron Microscopy Analysis

The surface (Figures 1a)-h)) and cross-sectional (Figures 2a)-d)) morphologies of the synthesized Sb_2S_3 thin films were characterized using scanning electron microscopy (SEM). Contrasting with the compact and continuous films seen in cross-sectional SEM, top-view images revealed a surface primarily composed of spherical particles. The SEM image of the film deposited for 5 hours revealed discontinuous film formation (Figure 1a)), whereas increasing the deposition time to 8 hours produced a compact and uniform surface (Figure 1b)). Films grown with longer deposition times (10 and 15 hours) exhibited additional hollow cone-like structures (Figures 1c)-d)). This indicates that deposition time significantly influences film morphology. Higher magnification images (Figures 1e)-h)) of the films grown with longer deposition times further illustrated the presence of inter-particle voids between larger spherical particles and the formation of hollow cone-like structures within them. The observed hollow cone-like structures within inter-particle voids were attributed to surface energy minimization. The limited space within the voids constrains Sb_2S_3 crystal growth, promoting a configuration that minimizes overall surface energy. This results in anisotropic growth, where crystals preferentially grow outwards, forming hollow cone-like structures. Consequently, the optimization of deposition time is critical for the fabrication of high-quality Sb_2S_3 films.

Using cross-sectional SEM, the film thicknesses of the samples were measured as 502 nm, 740 nm, 870 nm, and 1200 nm for S-5h, S-8h, S-10h, and S-15h, respectively. The thickness of the films exhibited a linear increase with respect to deposition time. As evidenced by EDS analysis (Table 1), the Sb/S atomic ratios of the films were in close alignment with the stoichiometric Sb_2S_3 composition of 1.5.

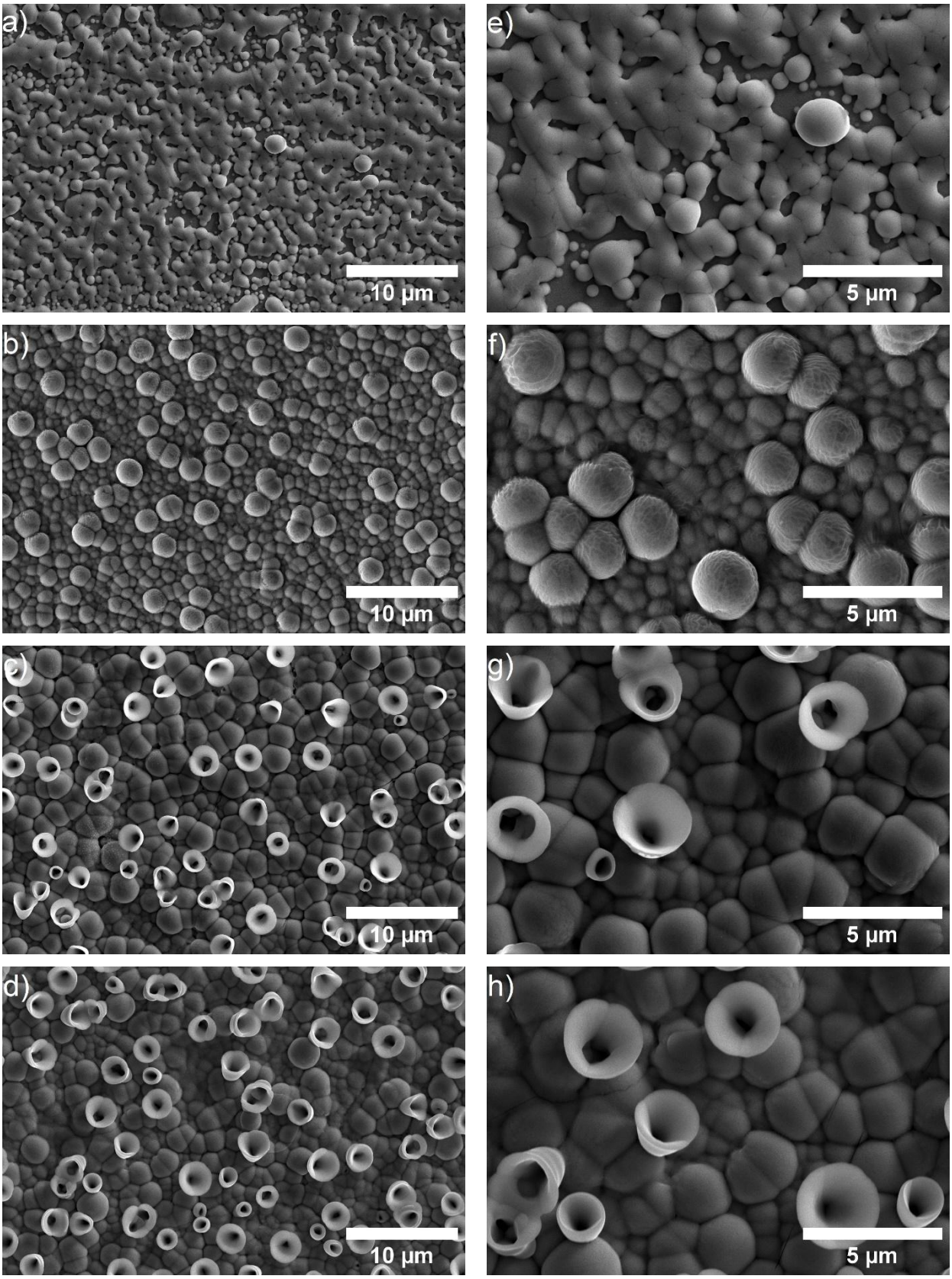

Figure 1. SEM images (10 kX magnification) of Sb_2S_3 thin films with varying deposition times are shown in a) S-5h, b) S-8h, c) S-10h, and d) S-15h. For detailed analysis, magnified SEM images (25 kX magnification) of the samples are presented in e) S-5h, f) S-8h, g) S-10h, and h) S-15h.

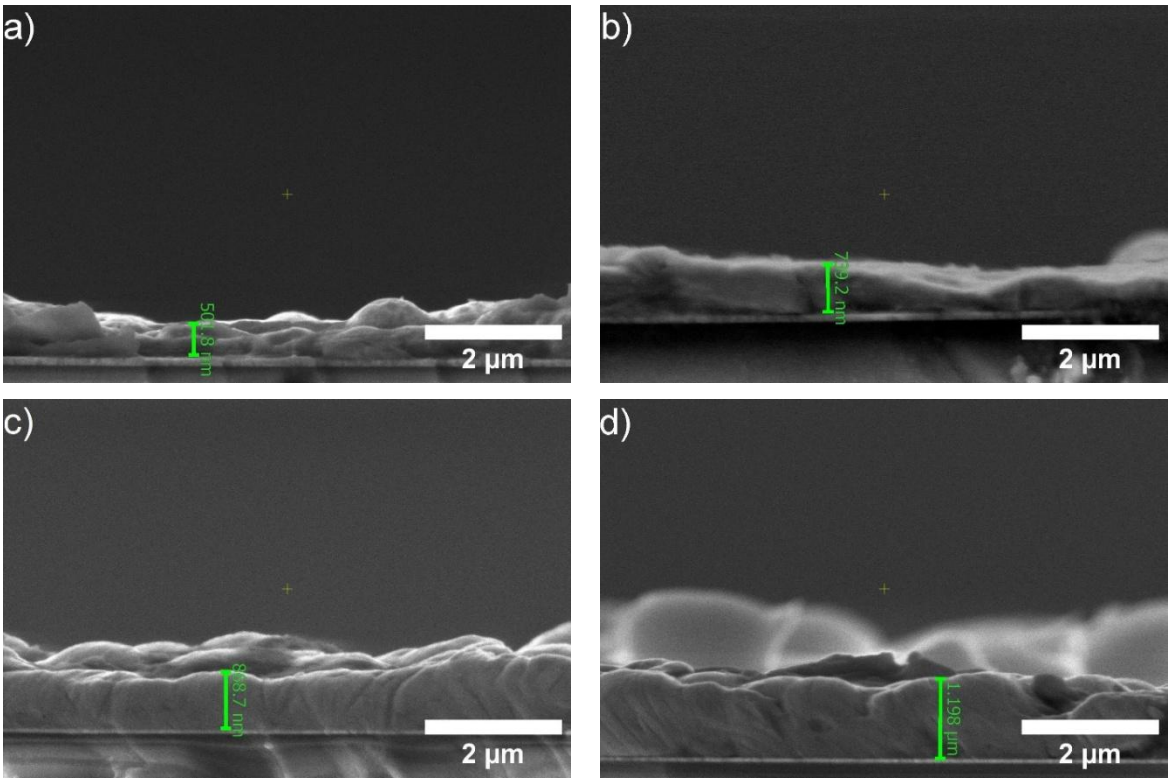

Figure 2. Cross-sectional SEM images (50 kX magnification) of Sb_2S_3 thin films fabricated with varying deposition times a) S-5h, b) S-8h, c) S-10h, and d) S-15h

Table 1. Average elemental compositions and thicknesses of the synthesized Sb_2S_3 thin films

Sample Name	[S] (Atomic %)	[Sb] (Atomic %)	S/Sb	Thickness (nm)
S-5h	59.17	40.83	1.45	502 ± 20
S-8h	59.46	40.54	1.47	740 ± 30
S-10h	59.83	40.17	1.49	870 ± 35
S-15h	59.71	40.29	1.48	1200 ± 48

3.2 X-Ray Diffraction Analysis

X-ray diffraction patterns (Figure 3) revealed the polycrystalline nature of the fabricated Sb_2S_3 thin films. The patterns matched the orthorhombic Sb_2S_3 phase (JCPDS #42-1393), with diffraction peaks at 2θ values of around 17.55°, 29.25°, 25.00°, 32.39°, 33.43°, which correspond to the (120), (211), (310), (221), and (301) planes, respectively. The synthesis of highly crystalline Sb_2S_3 thin films was confirmed by the presence of sharp diffraction peaks and the absence of peaks corresponding to impurities or secondary phases.

The crystallographic orientation of Sb_2S_3 thin films significantly influences solar cell performance by impacting charge carrier transport. In photovoltaic applications, vertical orientation, where the c-axis is perpendicular to the substrate, is considered advantageous for efficient charge carrier transport within the absorber layer (Tang et al., 2020; Turkoglu et al., 2022). A distinct relationship was found between deposition time and the preferred orientation of hydrothermally deposited Sb_2S_3 thin films. Specifically, longer deposition times led to (hk0) orientation, whereas shorter deposition times resulted in (hk1) orientation. Films synthesized for 5 and 8 hours exhibited preferential orientations of (221) and (211), respectively, whereas films synthesized for 10 and 15 hours demonstrated a preferential orientation of (310).

The preferred orientation of the samples was quantified using texture coefficients (TCs), which were calculated by the following equation and displayed in Figure 4.

$$TC_{(hkl)} = \frac{I_{(hkl)}}{I_{0(hkl)}} / \left(\frac{1}{N} \sum \frac{I_{(hkl)}}{I_{0(hkl)}} \right)$$

The variables in the formula are $I_{(hkl)}$ for measured peak intensity, $I_{0(hkl)}$ for reference peak intensity (JCPDS #42-1393), and N for the total number of reflections. TC provides a quantitative measure of the degree of preferred crystallographic orientation of crystallites along the (hkl) plane, where increased TC values indicate enhanced orientation. As illustrated in Figure 4, longer deposition times resulted in the most pronounced (hk0) preferred orientations, conversely, shorter deposition times resulted in the most pronounced (hk1) preferred orientations. Variations in deposition time can alter the balance of ions on the surface, potentially promoting the growth of planes with lower surface energies. Analysis of the TC(221)/TC(310) and TC(211)/TC(310) ratios (Figure 4b)) indicated maximum values for films deposited with shorter durations, demonstrating that deposition time can be used to control the formation of tilted $(Sb_4S_6)_n$ ribbons and achieve higher TC values for the (hk1) plane.

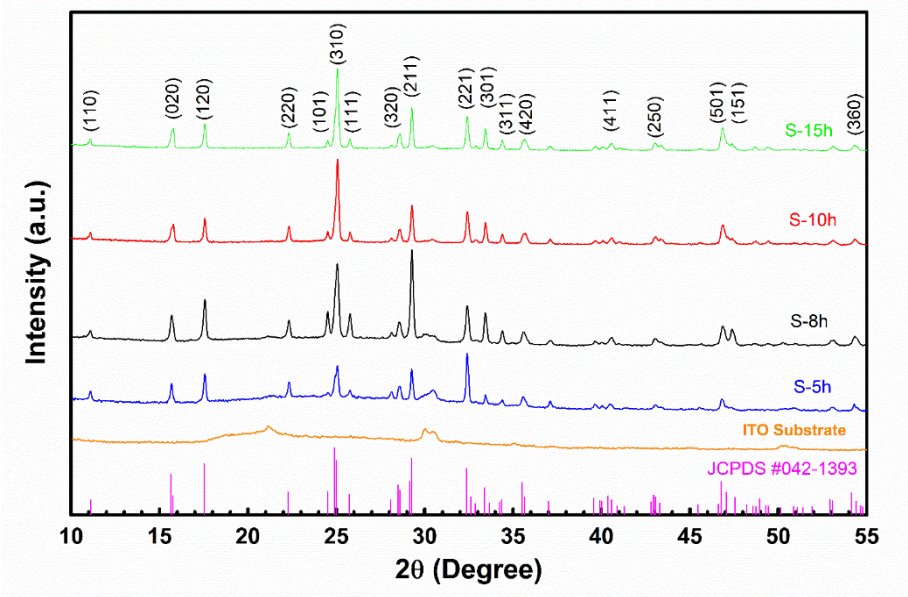

Figure 3. XRD spectra of annealed Sb_2S_3 thin films fabricated with varying deposition times a) S-5h, b) S-8h, c) S-10h, and d) S-15h

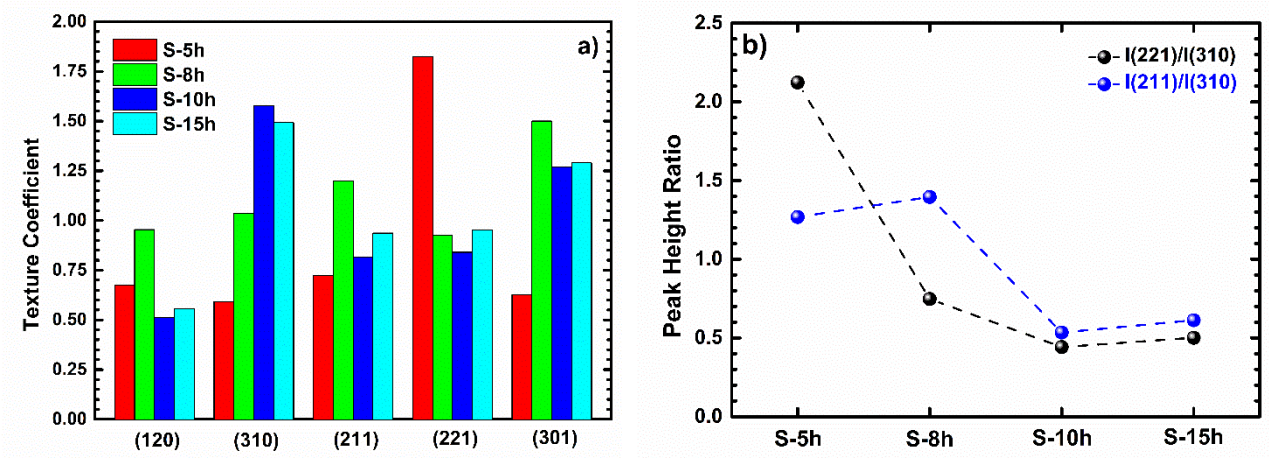

Figure 4. a) The texture coefficients (TC) of the diffraction patterns of the annealed Sb_2S_3 thin films fabricated with varying deposition times, b) The variation of the TC(211)/TC(310) and TC(221)/TC(310) ratio of the diffraction patterns

3.3 UV/VIS Spectrophotometer Analysis

By analyzing the UV-VIS transmission spectra of Sb_2S_3 thin films within the 500-1100 nm wavelength range (Figure 5a), their optical band gap energies were determined. Low transmission was consistently observed across all Sb_2S_3 films, with a further reduction in transmittance for films grown over longer durations. The very low transmission measured for the films suggests these films efficiently absorb a substantial portion of visible light. A two-step absorption edge was also observed in the S-5h film (inset of Figure 5a)), suggesting a discontinuous film structure that resulted in the combined absorption characteristics of ITO and S-5h. The optical band gap energies of the Sb_2S_3 thin films were determined via Tauc equation, $\alpha h\nu = A(h\nu - E_g)^{1/2}$, where α represents the absorption coefficient, hν is the photon energy, and A is a constant. Specifically, the band gaps were derived from the linear extrapolation of $(\alpha h\upsilon)^2$ vs. (hυ) plots (Figure 5b). Accurate bandgap determination for the S-5h film is hindered by its two-step absorption edge. The estimated band gaps for the S-8h, S-10h, and S-15h films (1.67 eV, 1.71 eV, and 1.73 eV, respectively) were in agreement with previously published results (Liu et al., 2016; Chen and Chen, 2020).

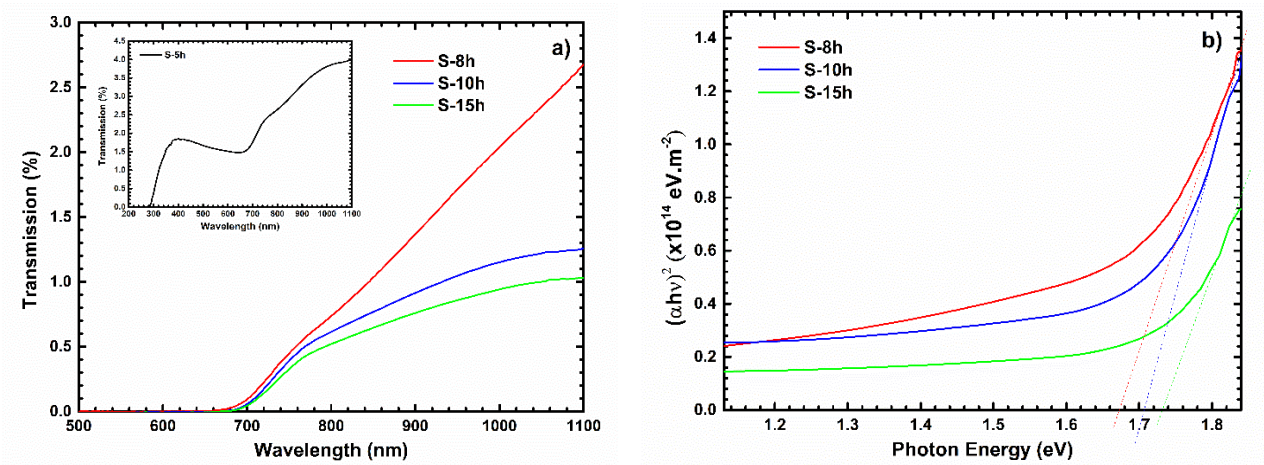

Figure 5. a) Transmission spectra (The inset graph displays the transmission spectrum of the S-5h sample) and b) Optical band gap energy plots for S-8h, S-10h, and S-15h samples

4. CONCLUSION

Hydrothermal deposition was employed to grow Sb_2S_3 thin films on ITO-coated glass substrates. The resulting films were then thoroughly characterized by SEM, XRD, and UV-VIS spectroscopy to determine the influence of deposition time on their crystal structure, morphology, and optical properties. Spherical particles were consistently observed on the surface of synthesized Sb_2S_3 samples in top-view SEM images, and continuous film formation was confirmed by cross-sectional SEM. Notably, longer deposition times (10 and 15 hours) led to hollow cone-like structures within inter-particle voids, which were attributed to surface energy minimization within the voids, while shorter times (5 and 8 hours) resulted in uniform surfaces. A clear relationship was observed between deposition time and the preferred orientation of Sb_2S_3 films. Longer deposition times resulted in (hk0) orientation, while shorter times yielded (hk1) orientation. The band gaps of the films remained relatively consistent across different deposition times. Optimization of the deposition time at 8 hours resulted in the successful synthesis of Sb_2S_3 films with a suitable band gap, compact surface morphology, and (hk1) preferred crystallographic orientation. In summary, deposition time strongly affects Sb_2S_3 film properties, requiring precise control for developing efficient Sb_2S_3 solar cells.

5. ACKNOWLEDGEMENTS

The author acknowledge the use of facilities provided by ISTE Center for Science and Technology Studies and Research (ISTE-CSTSR) for this research.

6. CONFLICT OF INTEREST

The Author approves that to the best of their knowledge, there is not any conflict of interest or common interest with an institution/organization or a person that may affect the review process of the paper.

7. AUTHOR CONTRIBUTION

Hasan KOSEOGLU has the full responsibility of the paper about determining the concept of the research, data collection, data analysis and interpretation of the results, preparation of the manuscript and critical analysis of the intellectual content with the final approval.

8. REFERENCES

Chen Z., Chen G., The effect of absorber thickness on the planar Sb_2S_3 thin film solar cell: Trade-off between light absorption and charge separation, Solar Energy 201, 323–329, 2020.

Deng H., Feng X., Zhu Q., Liu Y., Wang G., Zhang C., Zheng Q., Wu J., Wang W., Cheng S., 8.2%-Efficiency hydrothermal Sb_2S_3 thin film solar cells by two-step RTP annealing strategy, Science China Materials 67(11), 3666-3674, 2024.

Kondrotas R., Chen C., Tang J., Sb_2S_3 solar cells, Joule 2(5), 857-878, 2018.

Liu M., Gong Y., Li Z., Dou M., Wang F., A green and facile hydrothermal approach for the synthesis of high-quality semi-conducting Sb_2S_3 thin films, Applied Surface Science 387, 790–795, 2016.

Shockley W., Queisser H.J., The Shockley-Queisser limit, Journal of Applied Physics 32(3), 510-519, 1961.

Tang R., Wang X., Lian W., Huang J., Wei Q., Huang M., Yin Y., Jiang C., Yang S., Xing G., Chen S., Zhu C., Hao X., Green M. A., Chen T., Hydrothermal deposition of antimony selenosulfide thin films enables solar cells with 10% efficiency, Nature Energy 5, 587–595, 2020.

Turkoglu F., Ekren M.E., Cantas A., Yakinci K., Gundogan H., Koseoglu H., Aygun G., Ozyuzer L., Structural and optical characteristics of antimony selenosulfide thin films prepared by two-step method, Journal of the Korean Physical Society 81 (3), 278-284, 2022.

Vavale S. D., Pawar S. G., Deshmukh D. H., Deshmukh H.P., Hydrothermal method for Synthesis of different Nanostructure Metal Oxide thin film, International Journal of Innovative Knowledge Concepts 6(11), 126, 2018.

Wang, X., Tang, R., Jiang, C., Lian, W., Ju, H., Jiang, G., Li, Z., Zhu, C., Chen, T., 2020. Manipulating the Electrical Properties of $Sb_2(S,Se)_3$ Film for High-Efficiency Solar Cell. Adv. Energy Mater. 10, 2002341.

Yildirim, M. A., Tuna Yildirim, S., Cagirtekin, A. O., Karademir, M., Karaduman Er, I., Coskun, A., Ates, A., Acar, S., 2019. The effect of deposition time on the structural, morphological and H_2S gas sensing properties of the V_2O_5 nanostructures deposited by hydrothermal method. Journal of Materials Science: Materials in Electronics 30, 12215–12223.